Check for updates

Oxidorhenium(v) complexes of apigenin: a rare example of catalysis with *O,O*-bidentate ligands obtained from a naturally renewable resource†

Milan R. Milovanović,[a] Stefan R. Nikolić,[a] Antoine Dupé,[b] Jörg A. Schachner (ID) *[b] and Ljiljana E. Mihajlović*[a]

When Re(v) precursor [ReOCl$_3$(PPh$_3$)$_2$] (**P1**) is reacted with apigenin (H**L1**, Hapg), the flavone coordinates as an *O,O*-bidentate ligand *via* the deprotonated 5-OH group and its neighboring ketone to the Re center. Novel oxidorhenium(v) complex [ReOCl$_2$(PPh$_3$)(**L1**)] (**1**) was successfully synthesized in boiling acetone in sufficient yield. To increase the solubility of apigenin and its respective complexes, the other two −OH groups in the 7 and 4′-position of the apigenin structure were protected. To do so, well-established acetyl- and TBDMS- (*t*BuMe$_2$Si-) protecting groups were introduced to the apigenin frame, resulting in the novel ligands H**L2** and H**L3**, respectively. Resulting oxidorhenium(v) complexes [ReOCl$_2$(PPh$_3$) (**L2**)] (**2**) and [ReOCl$_2$(PPh$_3$)(**L3**)] (**3**) showed much increased solubilities in standard organic solvents. All three complexes **1**−**3** were subsequently tested in catalytic olefin epoxidation, which is the first time for a Re complex with an *O,O*-bidentate ligand. All three complexes showed activity for substrate cyclooctene, with complex **2** giving a high activity for such complexes (TON = 300). The novel ligands H**L2** and H**L3** as well as all three novel complexes **1**−**3** were fully characterized by NMR and IR spectroscopy, MS spectrometry and elemental analysis. In addition, the solid-state structures of H**L2**, H**L3** and **1**−**3** were determined by single-crystal X-ray diffraction analysis.

Introduction

The rich coordination chemistry of rhenium is based on a wide range of its oxidation states spanning from −1 to +7 due to its position in Group VII of the periodic table, where it combines properties of both early and late transition metals. The most investigated complexes in modern literature contain rhenium in the oxidation states of Re(I), Re(v) and Re(VII).[1] These coordination complexes showed a broad field of applications in homogenous catalysis,[2–4] bioinorganic and medicinal chemistry[5,6] as well as small molecule activation.[7] In parallel to the progress of Re synthetic chemistry grew its applicative potential. But among all applicative prospects, Re complexes have distinguished themselves either as radiopharmaceuticals for nuclear/bioimaging[6,8,9] or as efficient catalysts in homogeneous catalytic epoxidation of olefins, most prominently with the discovery of methyltrioxorhenium(VII) (MTO).[10]

The low oxidation state Re complexes have been primarily studied in the light of their favorable kinetic stability and good biodistribution, which enabled them to be used as photosensitizers and bioimaging agents.[9,11] They are typically stabilized by π-acceptor ligands such as CO, PR$_3$, and RCN. The most distinguished class is a Re(I) group of kinetically stable and inert compounds with the *fac*-[Re(CO)$_3$]$^+$ core, primarily reported by the group of Walter Hieber.[12] The well-established field of Re(I) carbonyl-containing complexes then triggered the development of Re complexes in higher oxidation states, dominantly Re(v) and Re(VII). A milestone work of Herrmann in 1991 put the focus on MTO due to its remarkable catalytic activity in olefin epoxidation and oxidation.[13] With turnover numbers (TONs) of over 20 000, MTO has been positioned as the most active Re-based epoxidation catalyst to date.[3] Yet, the compound manifested a major drawback due to the often-observed hydrolysis of acid-sensitive epoxides. To address this challenge, oxidorhenium(v) complexes with tetra- and bidentate Schiff-base ligands were suggested in Herrmann's research group as potential epoxidation catalysts.[14] Indeed, further efforts in the following two decades were directed toward developing oxidorhenium(v) compounds and their promotion as homogenous epoxidation catalysts of cyclooctene.[2,15]

Apigenin (4′,5,7-trihydroxyflavone, Hapg, H**L1**) is a naturally occurring, bioactive flavone-type of molecule, commonly

[a]*Innovation Center of the Faculty of Chemistry, Belgrade, Studentski trg 12–16, 11158 Belgrade, Serbia*

[b]*Institute of Chemistry, University of Graz, Schuberstr. 1, 8010 Graz, Austria*

present in a variety of fruits, vegetables, and medicinal plants. Its applicative potential is well-reported nowadays, especially having in mind its proven anti-allergic, antibacterial, anti-cancer, anti-inflammatory and antiviral effects.[16] There is a growing body of published research concerning flavonoid ligands in transition metal complexes,[17] but only a small number of them are apigenin complexes and none are of rhenium.[18] In many cases, full characterization or isolation of the reported coordination compounds is lacking, especially X-ray confirmation of the solid state structure. From a strictly chemical point of view, Hapg shares coordination features with the acac moiety (Fig. 1). However, in contrast to the large number of Re complexes with various N,O,[19] O,P,[20] or O,S and O,C[21] ligands, the chemistry with O,O[22] ligand donor sets is surprisingly scarce. So far, only a few Re-acetylacetonates (acac)[23] and related compounds[24] have been synthesized and structurally characterized. Also, to the best of our knowledge, such O,O-ligands have never been tested as epoxidation catalysts. These surprising gaps of knowledge further motivated us to investigate the naturally renewable molecule apigenin as a potential ligand for rhenium and the resulting chemistry of these complexes.

Within this publication, we report the synthesis and full characterization of the first three examples of oxidorhenium(v) complexes $[\mathrm{ReOCl_2PPh_3(L1\text{--}3)}]$ (1–3) containing the apigenin ligand HL1 and two newly synthesized apigenin derivatives HL2–3 (Fig. 1). To enhance the very low solubility of both apigenin HL1 and the resulting complexes 1, substituents on 4′-OH and 7-OH based on established protecting group chemistry (–OAc in HL2; –Si(tBu)Me$_2$ or TBDMS in HL3) were introduced. As part of these chemical investigations, the three new oxidorhenium(v) complexes 1–3 were tested in a classical chemical catalysis, namely olefin epoxidation.

Results and discussion

Apigenin (HL1) itself is only soluble in the strong polar solvents DMSO and DMF, and poorly soluble in acetone (Table 1), a phenomenon often observed in flavonoid chemistry.[25] This low solubility severely complicated synthesis of complexes, even more so as the use of DMSO was excluded because of reaction of these oxidorhenium(v) complexes with DMSO due to their Oxygen-Atom-Transfer (OAT) capabilities. Therefore,
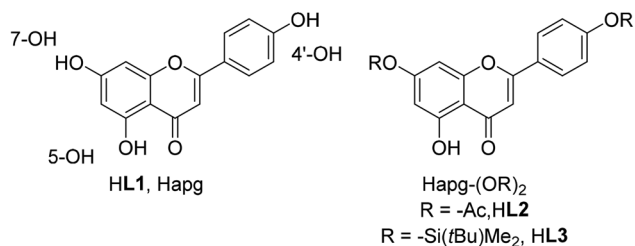
Table 1 Approximate solubilities (in mg ml^{-1}) of complexes 1–3

[mg ml^{-1}]	1	2	3
DMF	1.01	1.50	5.33
Acetone	0.31	1.38	9.86
THF	0.21	1.36	4.32
Acetonitrile	<0.05	1.01	5.56
MeOH	<0.05	<0.05	0.78
EtOH	<0.05	<0.05	<0.05
DCM	<0.05	4.47	4.46
Chloroform	<0.05	1.37	1.25
Diethylether	<0.05	<0.05	<0.05
Toluol	<0.05	<0.05	0.77

the synthesis of O-protected ligands HL2 and HL3 became necessary due to the low solubility of Apigenin HL1 (Fig. 1). For the synthesis of protected apigenin ligands HL2 and HL3, we turned to literature-established protocols. Acetylated ligand HL2 was synthesized via a modified Eichhorn acetylation[26] using acetic anhydride and pyridine as solvent, thereby avoiding purification by column chromatography. We had observed that HL2 is partly deprotected again on silica gel. Silylated ligand HL3 was synthesized by adopting a literature procedure using TBDMSCl and Et$_3$N in CH$_2$Cl$_2$.[27] After the reaction, the crude product was extracted with pentane to remove Et$_3$NCl. Single crystals of HL3 could also be grown from a concentrated pentane solution. Again, column chromatography was avoided, as partial hydrolysis of a silyl-protecting group did occur. In none of our experiments, the unwanted protection of the –OH group at the 5-position was observed, potentially due to a strong H-bond to the neighboring ketone and a resulting lower acidity at that position.

The synthesis of novel Re complexes 1–3 was achieved by reaction of the precursor complex $[\mathrm{ReOCl_3(PPh_3)_2}]$ (P1) and an equimolar amount of the respective ligand in boiling acetone. Reaction times of 1–2 hours were found to be enough to achieve a sufficient conversion (up to 80%). Here, the low solubility of parent apigenin HL1 in acetone required a pre-dissolution of HL1 in boiling acetone. To this solution, P1 was added and further heated to refluxing temperatures. For the more soluble ligands HL2 and HL3, the synthesis was started by mixing P1 and the respective ligand at 25 °C in acetone. The removal of the PPh$_3$ by-product was most effective via a short flash chromatography column in cyclohexane/ethyl acetate (see Experimental section). Single crystals of 1 were also obtained from that solvent mixture (Scheme 1).

Complex 1 showed the expected analytical data for an oxidorhenium(v) complex. Whereas the changes in the ^{1}H NMR spectrum between free ligand HL1 and complex 1 were the least pronounced of all the NMR data, the color of 1 was an unusual dark brown. Mostly, oxidorhenium(v) complexes are green, as are 2 and 3. The resonance for the coordinated PPh$_3$ ligand in 1 shifted significantly to higher field at −18.7 ppm (acetone-d_6), similar to other published Re(v) complexes.[28] The Re=O bond was found at 943 cm^{-1} in the typical region of the IR spectrum for such rhenium-oxo bonds. X-ray diffraction analysis also confirmed an octahedral cis-Cl,Cl arrangement

Fig. 1 Structure of apigenin HL1 showing the numbering of the 3 OH-groups; novel ligands HL2 and HL3.
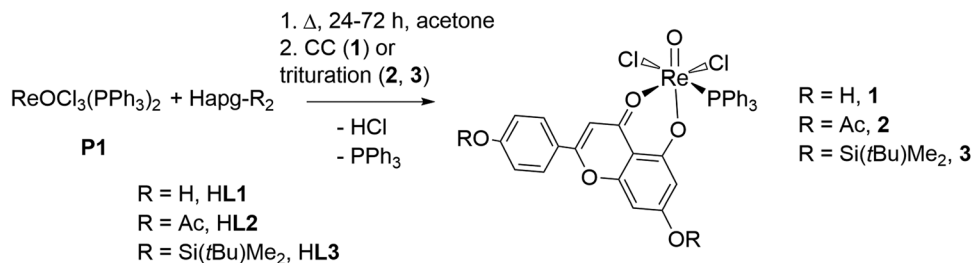
Scheme 1 Synthesis of complexes **1–3** (CC = column chromatography, cyclohexane, EtOAc 1/1). Yields: **1** – 52%, **2** – 57% and **3** – 73%.

around the Re center, with the phenolate-O atom of the **L1** moiety *trans* to the oxido ligand. Interestingly, the mass of **1** could not be measured by EI-MS, as only fragments even below the mass of H**L1** were obtained. Only with a soft ionization technique like ESI-MS, the mass spectrum of **1** could be obtained. Complex **2** was synthesized from **P1** and H**L2** in acetone, albeit here simple mixing at rt and then boiling for only 2 h was sufficient. The green crude product of **2** was most efficiently purified by trituration of concentrated crude solution in diethyl ether. Single crystals of **2** were obtained by re-crystallization from acetone (see Experimental section). Similar structural parameters than for **1** were also observed for **2**. The PPh$_3$ ligand resonated at −17.7 ppm in the ^{31}P NMR spectrum (acetone-d_6), and a meaningful MS could again only be acquired by ESI-MS. In the IR spectrum however, the Re=O bond was found at a rather unusual high shift of 980 cm^{-1}. X-ray diffraction analysis also confirmed an octahedral *cis*-Cl, Cl arrangement around the Re center, with the phenolate-O atom of the **L2** moiety *trans* to the oxido ligand. Complex **3** finally was synthesized under similar conditions as **2**. As complex **3** suffered from partial loss of the silyl protecting group on silica, excess PPh$_3$ could be removed by drop-wise addition of a concentrated crude solution of **3** in acetone into a large excess of *n*-pentane under fast stirring (trituration). A re-crystallization from acetone/diethylether finally yielded **3** in pure form. The coordinated PPh$_3$ ligand in **3** resonated at −18.7 ppm in the ^{31}P NMR spectrum (acetone-d_6), the two inequivalent silicon atoms of **3** were detected at 25.13 and 23.43 ppm in the ^{29}Si NMR spectrum. A meaningful mass spectrum could be acquired by ESI-MS. In the IR spectrum, the Re=O bond was found at 969 cm^{-1}. Complex **1** showed low to no solubility in the standard organic solvents, except for acetone, THF and DMF (Table 1). We assume this low solubility is due to an extended network of H-bridges that forms

between the two –OH groups present in the backbone of the apigenin moiety of complex **1**. In contrast to **1**, complexes **2** and **3**, where the –OH groups are protected, solubilities are largely increased in polar to medium polar solvents. An approximation of solubilities, done by visual checking of dissolution in the respective solvent, can be found in Table 1. All three complexes decompose in DMSO, most likely *via* OAT.

Solid state structures

As expected, there are no significant structural changes to the apigenin core in H**L2** and H**L3** (for structure discussion of ligands H**L2** and H**L3**, please see the ESI†) compared to H**L1** caused by the protecting groups (Table 2). The three bond lengths of the 5-OH group C1–O1 and its neighboring keto group C7–O2 are the same within experimental error.

Currently, complexes **1–3** are the first examples of Re-apigenin complexes characterized by single-crystal X-ray spectroscopy. All three complexes **1** (Fig. 2), **2** (Fig. 3) and **3** (Fig. 4) show a distorted octahedral coordination around the Re center in the solid state. The respective phenolate-oxygen of the apigenin moiety is located *trans* to the oxido ligand, and the two chlorido ligands are in *cis* orientation. Bond angles and distances for complexes **1–3** were all within expected range (Table 2, also see ESI†). Single crystals of **1** were obtained by re-crystallization from a cyclohexane/ethylacetate solvent mixture, of **2** from acetone and of **3** from acetone/diethylether. The presence of acetyl-groups in **2** or the TBDMS-groups in **3** does not affect the distorted octahedral geometry around the Re center. Also the bond lengths around Re are more less the same. The Re=O bond in **1** is somewhat elongated (1.712(2) Å) compared to **2** (1.6788(15) Å) and **3** (1.6814(17) Å) (Table 2). One structural feature of all three complexes is interesting to note, that is the now more similar bond lengths of Re1–O2 and Re1–O3 bonds. This proves a significant bond delocaliza-

Table 2 Selected bond distances [Å] and angles [°] for complexes **1–3**

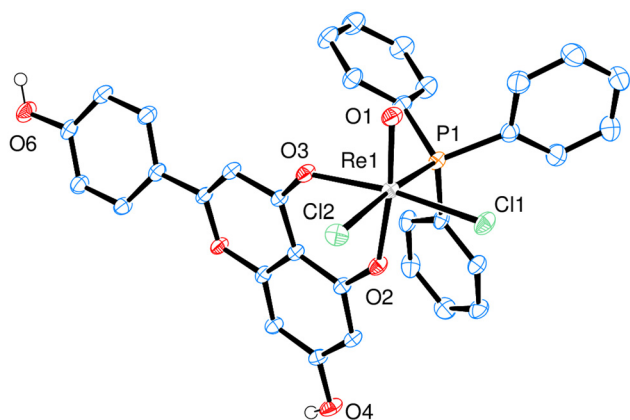| [Å]	Re1=O1	Re1–P1	Re1–Cl1	Re1–Cl2	Re1–O2	Re1–O3
1	1.709(2)	2.4626(8)	2.3361(7)	2.4260(7)	1.944(2)	2.088(2)
2	1.6788(15)	2.4482(5)	2.3441(5)	2.3986(5)	1.9912(14)	2.0765(14)
3	1.6814(17)	2.4597(6)	2.3488(6)	2.3995(6)	1.9741(15)	2.1051(16)
[°]	O1=Re1–O2	O1=Re1–P1	Cl1–Re1–Cl2			
1	168.94(9)	89.42(8)	90.98(3)			
2	166.61(7)	91.66(5)	89.605(18)			
3	166.14(8)	88.19(6)	87.89(2)			

Fig. 2 ORTEP plot (50% probability) of complex **1** (H atoms except for the 7-OH and 4'-OH groups are omitted).
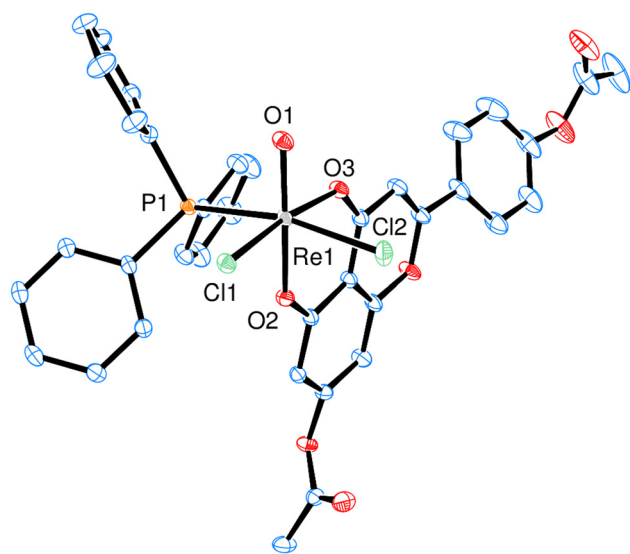

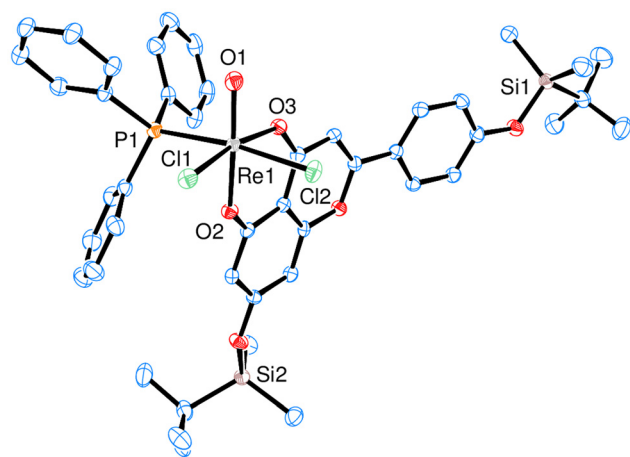**Fig. 3** ORTEP plot (50% probability) of complex **2** (H atoms are omitted for clarity).

Fig. 4 ORTEP plots (50% probability) of complex **3** (H atoms are omitted for clarity).

tion, as is also observed in an acac-chelate ring, in contrast to the initially localized C–OH single- and C=O double-bond of the respective apigenin ligands.

By close visual inspection of crystal packing of **HL2** one can recognize that most dominant non-covalent intermolecular interactions are stacking interactions between aromatic and resonance-assisted hydrogen-bridged (RAHB) rings, C–H⋯O (carbonyl) and C–H⋯π interactions. In case of **HL3** most dominant non-covalent intermolecular interactions are π⋯π stacking interactions, C–H⋯O and C–H⋯π interactions. The similar interactions seem to be important in crystal packing of the corresponding Rhenium(v) complexes. Namely, in the case of **1** non-covalent interactions that play a role in crystal packing are π⋯π stacking interactions, C–H⋯π interactions and hydrogen bonds (O–H⋯O and O–H⋯Cl); while in the case of **2** seemingly there is no stacking interactions, but C–H⋯π, C–H⋯O and C–H⋯Cl interactions; interactions with a co-crystalized molecules of chloroform represent a significant portion of intermolecular interaction in the case of **2**. In the case of **3** most dominant are π⋯π stacking and C–H⋯Cl interactions.

Epoxidation catalysis. Complexes **1–3** were tested in cyclooctene (**S1**) epoxidation using *tert*-butylhydroperoxide (TBHP, 5.5 M in decane) or hydrogen peroxide (H_2O_2, 30 vol%) as the oxidant. Under standard conditions, $CHCl_3$ was used as a solvent at 50 °C, with 1 mol% catalyst loading and 3 equiv. of oxidant. For complexes **2** and **3**, also 1-octene (**S2**) and styrene (**S3**) were tested as substrates (Scheme 2). Aliquots were withdrawn at given time intervals and the conversion to epoxide analyzed by GC-MS.

An overview of epoxidation results with **S1** is given in Table 3. In a first round of testing, all three complexes **1–3** showed activity for epoxidation of cyclooctene **S1** with *tert*-butylhydroperoxide (TBHP) as oxidant in chloroform, but with pronounced different activities (Fig. 5). Complex **1** showed the lowest activity with a TON = 46 over 24 h reaction time. This rather low activity can most likely be attributed to the low solubility of **1** in $CHCl_3$ (Table 1). After the 24 h experiment time, undissolved material of **1** was still visible in the reaction mixture. Under the same conditions, the fully dissolved complexes **2** and **3** showed a better reactivity. Complex **2** reached a TON of 73 after already four hours, **3** showed a similar activity
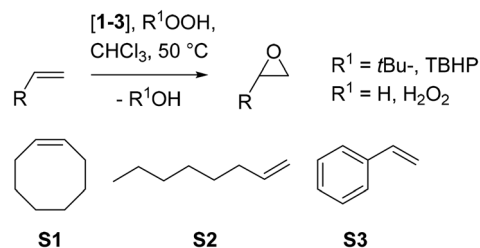
Scheme 2 Epoxidation catalysis with complexes **1–3** and olefinic substrates **S1–3**.
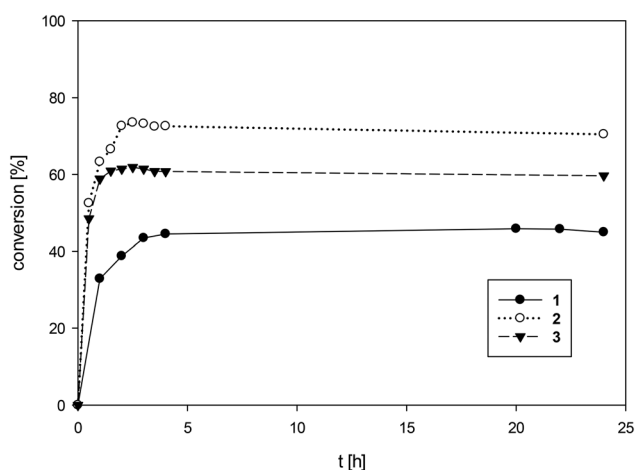
Table 3 Overview of TON (TOF, [h⁻¹]) of complexes **1–3** for cyclooctene **S1**

1 mol%	TBHP S1, CHCl₃	H₂O₂ S1, acetone	S1, CHCl₃
1	46 (1.9)	34 (1.4)	<10
2	73 (18.25)	28 (14)	<10
3	60 (15)	30 (3.75)	67 (22)

1 mol% catalyst loading, 50 °C; TOF in h⁻¹ at time of maximum conversion.

Fig. 5 Comparison of epoxidation activity of complexes **1–3** for cyclooctene **S1** (CHCl₃, 50 °C, 1 mol%, 3 equiv. TBHP).

to **2** reaching a TON of 60 after four hours. At a reduced catalyst loading of 0.1 mol%, complex **2** still gave 30% conversion to epoxide, resulting in a TON = 300.

In a second set of experiments, complexes **1–3** were tested with TBHP in acetone as a solvent. Caution has to be applied, as oxidizers and acetone can, in principle, form explosive acetone peroxides.[29] However, reactions were carried out under TBHP dilution, in the absence of protons and the reaction mixture was shaken, not stirred by magnetic stirring. Whereas the solubilities of **1–3** are higher in acetone compared to CHCl₃, the epoxidation activities were lower in all three cases (Table 3). Potentially, acetone is a too strongly coordinating solvent, which is able to compete with the TBHP for coordination on the Re center. In addition, complexes **2** and **3** were also tested in THF and MeOH, but both remained unreactive in these solvents. Probably, the donating nature of these solvents competes with TBHP for a coordination site on Re, thereby shutting down epoxidation activity.

In a second round of experiments, the aqueous oxidant H₂O₂ was tested for cyclooctene **S1**, as H₂O₂ is considered a greener oxidant compared to TBHP.[30] We hoped that the presence of two –OH groups in the ligand backbone of complex **1** would be beneficial for the use of aqueous oxidant H₂O₂. Tests were performed only in CHCl₃ as the mixture of acetone and H₂O₂ can lead to formation of explosive acetone peroxides.[29]

Somewhat surprisingly though, this time only complex **3**, with the silyl-protected apigenin backbone, showed a remarkable activity of TON = 67 (Table 3). Even at a lowered catalyst loading of 0.1 mol%, complex **3** still reached a conversion of 17%, equivalent to a TON = 170 with H₂O₂ as the oxidant.

For the other two substrates **S2–3**, complexes **1–3** showed the same unsatisfactory, but often observed catalyst profile. For 1-octene **S2**, low activities were observed, leaving the substrate more or less unchanged over 24 hours. Parent apigenin Re-complex **1** also showed no activity for the epoxidation of styrene **S3**, whereas acetylated and silylated complexes, **2** and **3**, respectively, completely over-oxidized **S3** to various products, mostly benzaldehyde. The non-reactivity of complex **1** for styrene **S3** is rather unusual for oxidorhenium(v) complexes.

As complexes **1–3** are the first examples of epoxidation catalysts containing an *O,O*-bidentate ligand, a comparison can only be made to other ligand systems of previously published oxidorhenium(v) catalysts [ReOCl₂(PPh₃)(**LL**)] (**LL** = monoanionic, bidentate ligand). The largest class of those catalysts does contain *O,N*-bidentate ligands and were reviewed in 2020 by Wolff and Machura.[2] Reported TONs for substrate **S1** for 22 catalysts ranged between 47–97, with the four most active ones containing ligands **LL¹**–**LL⁴** (Fig. 6).[31,32] Complexes [ReOCl₂(PPh₃)(**LL¹⁻³**)] also showed activity with aqueous H₂O₂ as oxidant (TON = 60, 53 and 74, respectively), albeit in 1,2-dichloroethane at 80 °C. In comparison, the TON of 67 for **3** achieved already at 50 °C (CHCl₃) can be considered to be a respectable result. The fantastic activities of MTO however (TON > 20 000)[3] also remain unchallenged by the three novel complexes reported herein.

The beneficial effect of ligands **LL¹⁻⁴** as well as the exact mechanism of Re(v) complexes *vs.* Re(vii) MTO-like complexes is still not fully understood. In general, the current mechanistic understanding follows the Sharpless mechanism of a concerted three component reaction between the complex, the oxidant and the olefin, where the olefin does not coordinate to the metal center.[33] Furthermore, the nature of the OAT is considered to be an electrophilic attack of the oxygen atom onto the olefin. Hence, any measures to enhance the electrophilicity of that coordinated oxygen atom before OAT should result in more active epoxidation catalysts and must therefore also be a result of the other coordinated ligands on the Re center. From our own research, we cannot conclude that a simple –I effect

	TON
ReOCl₂(PPh₃)(**LL¹**)	92
ReOCl₂(PPh₃)(**LL²**)	97
ReOCl₂(PPh₃)(**LL³**)	97
ReOCl₂(PPh₃)(**LL⁴**)	95

R = OMe, **LL¹**
R = Br, **LL²**
R = NO₂, **LL³**

LL⁴

Fig. 6 Three most active previously published ReOCl₂(PPh₃)(LL) complexes for **S1** epoxidation (1mol% cat., 50 °C, CHCl₃, 3 equiv. TBHP).

of the ligand is required, as the methoxy substituent in ligand moiety **LL**[1] should show a small +I effect. Potentially, it is the overall polarity of the ligands and the resulting complex that play a significant role for the concerted, three-membered Sharpless-type polar transition state. The three apigenin moieties **L1–3** described herein probably also exert an overall −I effect on the rhenium center, due to the presence of four oxygen atoms in the backbone and three aromatic phenyl rings. And complexes **1–3** are definitely highly polar molecules, as evidenced by their low solubilities in organic solvents. Overall, these semi-empirical guidelines should make up for an acceptable oxidorhenium(v) epoxidation catalysts, which was evidenced by the catalytic experiments.

Conclusions. The results presented here are the first examples of the synthesis of oxidorhenium(v) complexes equipped with a flavonoid-type, *O,O*-bidentate ligand and their use in epoxidation catalysis. The majority of epoxidation catalysts contain *O,N*-bidentate ligands.[15] Here, one general trend, that could be observed, was the beneficial influence of electron-withdrawing substituents and/or polarity of the complex on epoxidation activity.[31,34] The presence of a two aromatic ring systems and OH/alkoxide groups in the ligand backbone of **HL1** and **HL2–3**, respectively, overall effect a −I influence as a ligand. Complex **1** certainly suffers from its overall low solubility and hence results in lower catalytic activities. If the two remaining −OH groups of **1** are protected, both solubility as well as catalytic activity of resulting complexes **2** and **3** increase. Complex **3** in addition showed epoxidation activity with aqueous H_2O_2, also rarely observed for oxidorhenium(v) complexes.

Experimental section

General

Rhenium precursor $[ReOCl_3(PPh_3)_2]$ (**P1**) has been synthesized according to literature.[35] All other chemicals were purchased from commercial sources and were used without further purification. NMR spectra were recorded with a Bruker (300 MHz) instrument. Chemical shifts are given in ppm and are referenced to residual protons in the solvent. Signals are described as s (singlet), bs (broad singlet), d (doublet), dd (doublet of doublet), t (triplet), qd (quaternary doublet), m (multiplet) and coupling constants (J) are given in Hertz (Hz). Mass spectra were recorded with an Agilent 5973 MSD – Direct Probe using the EI ionization technique or HR-MS (ESI) measurements were recorded on an Agilent Technologies 6230 TOF LC/MS with ESI or APCI mass spectrometer in positive and negative ion mode, the used solvent was acetonitrile. Samples for infrared spectroscopy were measured on a Bruker Optics ALPHA FT-IR Spectrometer equipped with an ATR diamond probe head. GC-MS measurements were performed on an Agilent 7890 A with an Agilent 19091J–433 column coupled to a mass spectrometer type Agilent 5975 C. Elemental analyses were carried out using a Heraeus Vario Elementar automatic analyzer at the University of Technology Graz and performed in duplicate.

Crystal structures determination

Single-crystal X-ray data were obtained using a XtaLAB Synergy, Dualflex, HyPix-Arc 100 diffractometer (**HL2**, **HL3**, **3**) or a Bruker APEX-II CCD diffractometer (**1**) or a Bruker D8 Venture Photon II diffractometer (**2**). Reflection data were collected at $T = 100$ K using monochromatized Mo Kα radiation (**HL3**, **1**, **3**), Cu Kα radiation (**HL2**) or Ga Kα radiation (**2**). Data reduction, scaling and absorption corrections were performed using the CrysAlisPro software[35] (**HL2**, **HL3**, **3**) or APEX software[36] or APEX software[37] (**1**, **2**). For **HL2**, **HL3** and **3**, a numerical absorption correction based on Gaussian integration over a multifaceted crystal model and an empirical absorption correction using spherical harmonics, implemented in SCALE3 ABSPACK scaling algorithm of CrysAlisPro, were performed. For **1** and **2**, a semi-empirical absorption correction was performed using SADABS.[38]

The structures were solved with the ShelXT 2018/2[39] structure solution program using the intrinsic phasing solution method and by using Olex2[40] as the graphical interface. The models were refined with version 2019/3 of ShelXL[41] using full-matrix least-squares techniques against F^2. All non-hydrogen atoms were refined anisotropically. Hydrogen atom positions were calculated geometrically and refined using a riding model, except the H atoms of the OH groups which were found on a difference Fourier map and refined freely. For **HL2**, the O1–H1 distance was fixed at 0.88 Å with a DFIX constraint. For complex **3**, DFIX, SADI, RIGU, SIMU and SUMP constraints and restraints were used to model the disorder of the solvent molecules. For complex **2**, since the acetone solvent molecule lay on an inversion center and was disordered, the electron densities were removed from the electron density map by the SQUEEZE treatment using the OLEX2 solvent mask command. A solvent mask was calculated and 32 electrons were found in a volume of 222 Å^3 in 1 void per unit cell. This is consistent with the presence of 1 molecule acetone per unit cell ($Z = 2$), which accounts for 32 electrons.

CCDC 2407661 (**HL2**), 2407662 (**HL3**), 2407663 (**1**), 2407664 (**2**) and 2407665 (**3**)† contain the supplementary crystallographic data for this paper.

Epoxidation of cyclooctene. A Heidolph Parallel Synthesizer 1 was used for all epoxidation experiments. In a typical experiment, 2–3 mg of catalyst (1 mol%) were dissolved in 0.5 mL $CHCl_3$ and mixed with cyclooctene (1 equiv.), 50 μL of mesitylene (internal standard) and heated to the respective reaction temperature (50 °C). Then the oxidant (3 equiv.) was added. Aliquots for GC-MS (20 μL) were withdrawn at given time intervals, quenched with MnO_2 and diluted with HPLC grade ethyl acetate. The reaction products were analysed by GC-MS (Agilent 7890 A with an Agilent 19091J-433 column coupled to a mass spectrometer type Agilent 5975 C), and the epoxide produced from each reaction mixture was quantified *vs.* mesitylene as the internal standard. Experimental error of GC-MS measurements is ±5%.

Synthesis of Hapg(OAc)₂ HL2. Apigenin **HL1** (2.7 g, 10 mmol) was dissolved in pyridine (40 mL). To the yellowish

mixture Ac_2O (0.735 mL, 7.77 mmol) was added and allowed to stir for 3 h at room temperature. The mixture was poured in 100 ml of 10% HCl. The formed precipitate was filtered and washed with saturated solution of $NaHCO_3$, water and dried. The pure product of H**L2** was obtained as pale-yellow solid. Yield 3.27 g (95%). ^1H NMR (300 MHz, Acetone-d_6) δ 12.89 (s, 1H, –OH), 8.20–8.15 (m, 2H, 3'/5'-H) 7.42–7.35 (m, 2H, 2'/6'-H), 7.01 (d, J = 2.1 Hz, 1H, 4-H), 6.93 (s, 1H, 8-H), 6.60 (d, J = 2.1 Hz, 1H, 2-H), 2.31 (s, 3H, –C(O)CH$_3$), 2.30 (s, 3H, –C(O)CH$_3$). ^{13}C NMR (75 MHz, Acetone-d_6) δ 169.49, 162.70, 157.50, 129.04 (3'/5'-C), 123.69 (2'/6'-C), 106.69 (4-C), 106.31 (8-C), 102.30 (2-C), 21.13 (–C(O)CH$_3$). IR (ν, wavenumber cm^{-1}): 3089.73 (w, O–H), 3076 (w, C–H aromatic), 1754 (m, C=O ester), 1649.80 (s, C=O carbonyl), 1614.86 (s, C=C), 1592.02 (m, C=C aromatic), 1488.38 (m, C=C aromatic), 1367.75 (m), 1338.08 (m), 1289.10 (m), 1216.15 (m), 1189.54 (s, O–H), 1169.38 (s), 1134.80 (s), 1109.57 (m), 1017.65 (s), 920.59 (m), 894.25 (m), 822.85 (m), 714.16 (m), 626.60 (m), 585.54 (w), 500.17 (w), 460.14 (w), 421.01 (w); EI-MS: 354.2 (M$^+$); Elemental analysis calculated for $C_{19}H_{14}O_7$ (354.3 g mol^{-1}): calc. C 64.41%, H 3.98%; found: C 63.75%, H 3.79%.

Synthesis of Hapg(Si)$_2$ HL3. Apigenin H**L1** (1.35 g, 5 mmol, 1 equiv.) was suspended in CH_2Cl_2 (50 mL). To the yellowish mixture triethylamine (1.8 mL, 12.5 mmol, 2.5 equiv.) and *tert*-butyldimethylsilyl-chloride (TBDMSCl) (2 g, 13.27 mmol, 2.65 equiv.) were added and the reaction mixture was allowed to stir at room temperature. After 2 hours, all solvent was evaporated and the reaction mixture was dissolved in *n*-pentane (app.120 mL). Upon standing for 24 h, the side-product Et_3HNCl precipitated and was filtered off. After removal of *n*-pentane, pure H**L3** was obtained as a yellowish powder. Yield: 2.07 g (4.15 mmol, 83%). Single-crystals suitable for X-ray diffraction analysis were obtained by recrystallization from *n*-pentane. ^1H NMR (300 MHz, Acetone-d_6) δ 12.93 (s, 1H, OH), 8.04–7.98 (m, 2H, 3'/5'-H), 7.10–7.03 (m, 2H, 2'/6'-H), 6.71 (s, 1H, 8-H), 6.62 (d, J = 2.1 Hz, 1H, 4-H), 6.27 (d, J = 2.2 Hz, 1H, 2-H), 1.03 (s, 9H, *t*Bu), 1.02 (s, 9H, *t*Bu), 0.31 (s, 6H, 2 × CH$_3$), 0.30 (s, 6H, 2xCH$_3$); ^{13}C NMR (75 MHz, Acetone-d_6) δ 183.42, 165.11, 163.27, 163.14, 160.31, 129.39 (3'/5'-C), 125.28 (2'/6'-C), 121.66, 105.07 (8-C), 104.40 (2-C), 99.67 (4-C), 26.12 (*t*Bu), 26.06 (*t*Bu), 19.01 (*t*Bu), 18.99 (*t*Bu), −4.13 (CH$_3$), −4.15 (CH$_3$); ^{29}Si NMR (79 MHz, Acetone-d_6) δ 24.08, 23.07; IR (ν, wavenumber cm^{-1}): 2954.41 (w, C–H aliphatic), 2883.80 (w, C–H aliphatic), 1652.52 (m, C=O carbonyl), 1598.57 (m, C=C aromatic), 1507.90 (m, C=C aromatic), 1422.46 (m), 1340.58 (m), 1264.31 (s, Si–O), 1158.64 (s, O–H), 1113.05 (s), 1097.08 (w), 1029.39 (w), 983.93 (s), 908.62 (s), 825.21 (s), 781.42 (s), 711.25 (s), 674.09 (w), 546.30 (w), 479.09 (w); EI-MS: 498.5 (M$^+$); Elemental Analysis calculated for $C_{27}H_{38}O_5Si_2$ (498.77 g mol^{-1}): calc. C 65.02%, H 7.68%; found: C 64.72%, H 7.69%.

Synthesis of [ReOCl$_2$(PPh$_3$)(L1)] (1). Ligand H**L1** (0.27 g, 1.0 mmol, 1 equiv.) and acetone (300 mL) were mixed and heated to refluxing temperatures for one hour. To the yellowish mixture rhenium precursor [ReOCl$_3$(PPh$_3$)$_2$] (**P1**) (0.833 g, 1.0 mmol, 1 equiv.) was added and the reaction mixture was heated for 2 hours. After cooling down, the greenish reaction solution was concentrated to app. 10 mL and filtered through a Celite plug. The greenish-brownish filtrate containing **1** was purified by automated column chromatography using cyclohexane/ethylacetate as eluents (gradient from v/v 80/20 to 45/55). The greenish-brownish band was collected (at cyclohexane/ethylacetate v/v 45/55) and left for slow crystallization. After one day crystals were collected and dried to give 420 mg of complex **1** (0.52 mmol, 52%). Crystals suitable for X-ray diffraction analysis were grown from cyclohexane/ethyl acetate (45/55). ^1H NMR (300 MHz, Acetone-d_6) δ 9.87 (s, 1H, OH), 9.40 (s, 1H, OH), 7.98 (d, J = 8.8 Hz, 2H, 3'/5'-H), 7.67–7.39 (m, 15H, PPh$_3$), 7.09 (d, J = 8.8 Hz, 2H, 2'/6'-H), 7.01 (s, 1H, 8-H), 6.51 (d, J = 2.2 Hz, 1H, 4-H), 5.98 (d, J = 2.2 Hz, 1H, 2-H); ^{13}C NMR: no meaningful spectra could be obtained due to the low solubility of the complex in CDCl$_3$ and acetone-d_6; ^{31}P NMR (121 MHz, Acetone-d_6) δ −18.72; IR (ν, wavenumber cm^{-1}) 3448 (w, O–H), 3192 (w, O–H), 1626 (s, C=O carbonyl), 1581 (s, C=C aromatic), 1528 (s), 1499 (s), 1435 (m), 1359 (m), 1242 (m), 1167 (s), 1129 (m), 943 (s, Re=O), 846 (m), 824 (m), 690 (m, Re-P), 676 (m), 528 (s), 510 (s), 496 (s); (+)ESI-MS: 804.0 (M$^+$); Elemental Analysis calculated for $C_{33}H_{24}Cl_2O_6PRe$ (804.6 g mol^{-1}): C 49.26%, H 3.18%; found: C 49.19%, H 2.96%.

Synthesis of [ReOCl$_2$(PPh$_3$)(L2)] (2). Ligand H**L2** (0.35 g, 1.0 mmol, 1 equiv.) and [ReOCl$_3$(PPh$_3$)$_2$] (**P1**) (0.83 g, 1.0 mmol, 1 equiv.) were mixed in acetone (300 mL) and heated to refluxing temperatures for 2 hours. After cooling down, the greenish reaction solution was concentrated to app. 10 mL and filtered through a Celite plug. The filtrate was then triturated in 100 mL of *n*-pentane, allowing it to stir for 15–20 minutes. Removal of solvents and drying of the solid yielded 510 mg of complex **2** (0.57 mmol, 57%). Crystals suitable for X-ray diffraction analysis were grown from acetone. ^1H NMR (300 MHz, Acetone-d_6) δ 8.21 (d, J = 8.9 Hz, 2H, 3'/5'-H), 7.67–7.54 (m) and 7.50–7.40 (m, 12H, PPh$_3$ and 2'/6'-H), 7.38 (s, 1H, 8-H), 6.97 (d, J = 2.1 Hz, 1H, 4-H), 6.37 (d, J = 2.1 Hz, 1H, 2-H), 2.34 (s, 3H, C(O)CH$_3$), 2.28 (s, 3H, C(O)CH$_3$); ^{13}C NMR (75 MHz, Acetone-d_6) δ 168.83, 159.28, 155.91, 135.22, 135.09 (PPh$_3$), 132.33, 132.32, 129.83 (3'/5'-C), 129.73 (2'/6'-C), 129.59 (PPh$_3$), 123.62 (PPh$_3$), 109.51 (2-C), 106.43 (8-C), 102.6 (4-C), 21.0 (C(O)CH$_3$); ^{31}P NMR (121 MHz, Acetone-d_6) δ −17.11; IR (ν, wavenumber cm^{-1}): 3081 (w, C–H aromatic), 1757 (m, C=O ester), 1622 (m, C=O carbonyl), 1540 (m, C=C aromatic), 1423 (m), 1341 (w), 1193 (s), 1169 (s), 1138 (s), 1094 (s), 1005 (s), 980 (s, Re=O), 758 (m), 690 (m, Re–P), 529 (m), 509 (m); (+)ESI-MS: 852.9 (M$^+$ − Cl$^-$ − H$^+$); Elemental Analysis calculated for $C_{37}H_{28}Cl_2O_8PRe$ (888.7 g mol^{-1}): C 50.01%, H 3.18%; found: C 49.19%, H 2.96%.

Synthesis of [ReOCl$_2$(PPh$_3$)(L3)] (3). Ligand H**L3** (0.5 g, 1.0 mmol, 1 equiv.) and [ReOCl$_3$(PPh$_3$)$_2$] (**P1**) (0.83 g, 1.0 mmol, 1 equiv.) were mixed in acetone (350 mL) and heated to refluxing temperatures for 2 hours. After cooling down, the greenish reaction solution was concentrated to app. 10 mL and filtered through a Celite plug. The filtrate was then triturated in 100 mL of *n*-pentane, allowing it to stir for 15–20 minutes. A removal of solvents and drying of the solid

yielded 750 mg of complex **3** (0.73 mmol, 73%). Crystals suitable for X-ray diffraction analysis were grown from acetone/diethyl ether. ^{1}H NMR (300 MHz, Acetone-d_6) δ 7.94 (d, J = 8.8 Hz, 1H, 3′/5′-H), 7.56–7.43 (m) and 7.40–7.24 (m, 10H, PPh$_3$), 7.04 (d, J = 8.8 Hz, 2H, 2′/6′-H), 6.98 (s, 1H, 8-H), 6.48 (d, J = 2.2 Hz, 1H, 4-H), 5.95 (d, J = 2.2 Hz, 1H, 2-H), 0.93 (s, 9H, tBu), 0.86 (s, 9H, tBu), 0.22 (s, 6H, 2xCH$_3$), 0.15 (s, 3H, CH$_3$), 0.12 (s, 3H, CH$_3$); ^{13}C NMR (75 MHz, Acetone-d_6) δ 180.38, 165.07, 164.97, 161.09, 159.96, 159.17, 135.20 (PPh$_3$), 135.07 (PPh$_3$), 132.18 (PPh$_3$), 131.92 (PPh$_3$), 131.24 (PPh$_3$), 130.14 (3′/5′-C), 129.63, 129.49, 123.43, 121.49 (2′/6′-C), 107.65 (2-C), 104.83, 100.42 (4-C), 25.93 (tBu), 25.85 (tBu), 18.87 (tBu), 18.85 (tBu), −4.27 (CH$_3$), −4.34 (CH$_3$); ^{31}P NMR (121 MHz, Acetone-d_6) δ −18.86; ^{29}Si NMR (79 MHz, Acetone-d_6) δ 25.13, 23.43; IR (ν, wavenumber cm^{-1}): 3058 (w, C–H aromatic), 2928 (w, C–H aliphatic), 2855 (w, C–H aliphatic), 1738 (w), 1621 (s, C=O carbonyl), 1587 (s), 1483 (m), 1352 (m), 1244 (m, Si–O), 1173 (s), 1096 (m), 1038 (m), 969 (s, Re=O), 904 (m), 827 (s), 782 (s), 691 (s, Re-P), 526 (s), 508 (m); (+)ESI-MS: 1034 (M$^+$); Elemental Analysis calculated for: C 52.31%, H 5.07%; found: C 51.46%, H 4.89%.

Author contributions

The manuscript was written through contributions of all authors.

Conflicts of interest

The authors declare no competing financial interests.

Data availability

Data for this article, including files for NMR, IR and mass spectroscopic data, are available at Zenodo at https://zenodo.org/uploads/14883918; https://doi.org/10.5281/zenodo.14883918.

Acknowledgements

References

1 J. R. Dilworth, *Coord. Chem. Rev.*, 2021, **436**, 213822.
2 M. Wolff and B. Machura, *Rev. Inorg. Chem.*, 2020, **40**, 47–73.
3 J. W. Kück, R. M. Reich and F. E. Kühn, *Chem. Rec.*, 2016, **16**, 349–364.
4 (*a*) F. E. Kühn, *J. Organomet. Chem.*, 2023, 122824; (*b*) S. C. A. Sousa and A. C. Fernandes, *Coord. Chem. Rev.*, 2015, **284**, 67–92.
5 (*a*) E. B. Bauer, A. A. Haase, R. M. Reich, D. C. Crans and F. E. Kühn, *Coord. Chem. Rev.*, 2019, **393**, 79–117; (*b*) P. V. Simpson, N. M. Desai, I. Casari, M. Massi and M. Falasca, *Future Med. Chem.*, 2019, **11**, 119–135; (*c*) C. C. Konkankit, S. C. Marker, K. M. Knopf and J. J. Wilson, *Dalton Trans.*, 2018, **47**, 9934–9974; (*d*) A. Leonidova and G. Gasser, *ACS Chem. Biol.*, 2014, **9**, 2180–2193.
6 M. A. Klenner, T. Darwish, B. H. Fraser, M. Massi and G. Pascali, *Organometallics*, 2020, **39**, 2334–2351.
7 (*a*) W. Guan, F. B. Sayyed, G. Zeng and S. Sakaki, *Inorg. Chem.*, 2014, **53**, 6444–6457; (*b*) L. Alig, K. A. Eisenlohr, Y. Zelenkova, S. Rosendahl, R. Herbst-Irmer, S. Demeshko, M. C. Holthausen and S. Schneider, *Angew. Chem., Int. Ed.*, 2021, **61**, e202113340; (*c*) I. Klopsch, M. Finger, C. Würtele, B. Milde, D. B. Werz and S. Schneider, *J. Am. Chem. Soc.*, 2014, **136**, 6881–6883; (*d*) Q. J. Bruch, G. P. Connor, C.-H. Chen, P. L. Holland, J. M. Mayer, F. Hasanayn and A. J. M. Miller, *J. Am. Chem. Soc.*, 2019, **141**, 20198–20208; (*e*) J. L. Smeltz, P. D. Boyle and E. A. Ison, *J. Am. Chem. Soc.*, 2011, **133**, 13288–13291.
8 S. Hostachy, C. Policar and N. Delsuc, *Coord. Chem. Rev.*, 2017, **351**, 172–188.
9 J. J. Wilson, in *Biomedical applications of inorganic photochemistry*, ed. P. C. Ford and R. van Eldik, Academic Press, Cambridge, MA, San Diego, CA, Oxford, London, 2022, p. 1.
10 (*a*) W. A. Herrmann, *J. Organomet. Chem.*, 1995, **500**, 149–173; (*b*) F. E. Kühn, A. Scherbaum and W. A. Herrmann, *J. Organomet. Chem.*, 2004, **689**, 4149–4164.
11 (*a*) E. Wolcan, *Inorg. Chim. Acta*, 2020, **509**, 119650; (*b*) J. Palion-Gazda, K. Choroba, A. M. Maroń, E. Malicka and B. Machura, *Molecules*, 2024, **29**, 1631.
12 (*a*) W. Hieber, in *Advances in organometallic chemistry*, ed. F. A. Stone and R. West, Elsevier, Burlington, 1970, pp. 1; (*b*) W. A. Herrmann, *J. Organomet. Chem.*, 1990, **383**, 21–44; (*c*) J. E. Ellis and W. Beck, *Angew. Chem., Int. Ed. Engl.*, 1995, **34**, 2489–2491.
13 W. A. Herrmann, R. W. Fischer and D. W. Marz, *Angew. Chem., Int. Ed. Engl.*, 1991, **30**, 1638–1641.
14 (*a*) W. A. Herrmann, M. U. Rauch and G. R. J. Artus, *Inorg. Chem.*, 1996, **35**, 1988–1991; (*b*) F. E. Kühn, M. U. Rauch, G. M. Lobmaier, G. R. J. Artus and W. A. Herrmann, *Chem. Ber.*, 1997, **130**, 1427–1431.
15 B. Machura, M. Wolff and I. Gryca, *Coord. Chem. Rev.*, 2014, **275**, 154–164.

16 (a) D. Patel, S. Shukla and S. Gupta, *Int. J. Oncol.*, 2007, 233–245; (b) R. Liu, H. Zhang, M. Yuan, J. Zhou, Q. Tu, J.-J. Liu and J. Wang, *Molecules*, 2013, **18**, 11496–11511.

17 (a) E. Halevas, B. Mavroidi, G. Zahariou, M. Pelecanou and A. G. Hatzidimitriou, *Inorg. Chim. Acta*, 2023, **546**, 121325; (b) A. Yang, C. Liu, H. Zhang, J. Wu, R. Shen and X. Kou, *Eur. J. Med. Chem.*, 2022, **233**, 114216; (c) E. Halevas, B. Mavroidi, M. Pelecanou and A. G. Hatzidimitriou, *Inorg. Chim. Acta*, 2021, **523**, 120407; (d) M. Kozsup, X. Zhou, E. Farkas, A. C. Bényei, S. Bonnet, T. Patonay, K. Kónya and P. Buglyó, *J. Inorg. Biochem.*, 2021, **217**, 111382; (e) E. Halevas, A. Pekou, R. Papi, B. Mavroidi, A. G. Hatzidimitriou, G. Zahariou, G. Litsardakis, M. Sagnou, M. Pelecanou and A. A. Pantazaki, *J. Inorg. Biochem.*, 2020, **208**, 111083; (f) K. Karami, Z. Mehri Lighvan, H. Farrokhpour, M. Dehdashti Jahromi and A. A. Momtazi-Borojeni, *J. Biomol. Struct. Dyn.*, 2018, **36**, 3324–3340; (g) Y. Liu and M. Guo, *Molecules*, 2015, **20**, 8583–8594; (h) Z.-T. Zhang and J. Shi, *J. Coord. Chem.*, 2007, **60**, 1485–1491; (i) Y. He, *Acta Crystallogr., Sect. C: Cryst. Struct. Commun.*, 2006, **62**, m469–m471; (j) A.-C. Munteanu, A. Notaro, M. Jakubaszek, J. Cowell, M. Tharaud, B. Goud, V. Uivarosi and G. Gasser, *Inorg. Chem.*, 2020, **59**, 4424–4434; (k) X. Han, M. R. Kumar, A. Hoogerbrugge, K. K. Klausmeyer, M. M. Ghimire, L. M. Harris, M. A. Omary and P. J. Farmer, *Inorg. Chem.*, 2018, **57**, 2416–2424; (l) S. Roy, R. Das, B. Ghosh and T. Chakraborty, *Mol. Carcinog.*, 2018, **57**, 700–721; (m) D. Ravishankar, M. Salamah, A. Attina, R. Pothi, T. M. Vallance, M. Javed, H. F. Williams, E. M. S. Alzahrani, E. Kabova, R. Vaiyapuri, K. Shankland, J. Gibbins, K. Strohfeldt, F. Greco, H. M. I. Osborn and S. Vaiyapuri, *Sci. Rep.*, 2017, **7**, 5738.

18 (a) M. Khater, D. Ravishankar, F. Greco and H. M. Osborn, *Future Med. Chem.*, 2019, **11**, 2845–2867; (b) G. Erdogan, R. Karadag and A. Eler, *Main Group Met. Chem.*, 2010, **33**, 283–299; (c) M. Tan, J. Zhu, Y. Pan, Z. Chen, H. Liang, H. Liu and H. Wang, *Bioinorg. Chem. Appl.*, 2009, **2009**, 347872; (d) J. J. Martínez Medina, L. G. Naso, A. L. Pérez, A. Rizzi, N. B. Okulik, E. G. Ferrer and P. A. Williams, *J. Photochem. Photobiol., A*, 2017, **344**, 84–100.

19 (a) V. S. Sergienko, *Russ. J. Inorg. Chem.*, 2019, **64**, 583–591; (b) V. S. Sergienko and A. V. Churakov, *Russ. J. Inorg. Chem.*, 2018, **63**, 631–641; (c) V. S. Sergienko and A. V. Churakov, *Russ. J. Inorg. Chem.*, 2018, **63**, 753–763.

20 V. S. Sergienko and A. V. Churakov, *Russ. J. Inorg. Chem.*, 2017, **62**, 1327–1342.

21 V. S. Sergienko, *Russ. J. Inorg. Chem.*, 2017, **62**, 751–759.

22 (a) V. S. Sergienko and A. V. Churakov, *Russ. J. Inorg. Chem.*, 2016, **61**, 1708–1726; (b) C. Scholtysik, C. Njiki Noufele, A. Hagenbach and U. Abram, *Inorg. Chem.*, 2019, **58**, 5241–5252.

23 (a) C. J. L. Lock and C. Wan, *Can. J. Chem.*, 1975, **53**, 1548–1553; (b) M. Irmler and G. Meyer, *Z. Naturforsch., B:* *J. Chem. Sci.*, 1990, **45**, 1103–1104; (c) A. Brink, H. G. Visser and A. Roodt, *Acta Crystallogr., Sect. E:Struct. Rep. Online*, 2010, **67**, m34–m35.

24 C. Triantis, T. Tsotakos, C. Tsoukalas, M. Sagnou, C. Raptopoulou, A. Terzis, V. Psycharis, M. Pelecanou, I. Pirmettis and M. Papadopoulos, *Inorg. Chem.*, 2013, **52**, 12995–13003.

25 (a) L. Wei, J. Zhao, Y. Meng, Y. Guo and C. Luo, *LWT*, 2020, **118**, 108874; (b) F. J. Osonga, J. O. Onyango, S. K. Mwilu, N. M. Noah, J. Schulte, M. An and O. A. Sadik, *Tetrahedron Lett.*, 2017, **58**, 1474–1479; (c) Q.-Q. Wang, J.-B. Shi, C. Chen, C. Huang, W.-J. Tang and J. Li, *Bioorg. Med. Chem. Lett.*, 2016, **26**, 1460–1465.

26 *In Comprehensive organic name reactions and reagents*, ed. Z. Wang, Wiley, Chichester, pp. 967.

27 C. Qi, Y. Xiong, V. Eschenbrenner-Lux, H. Cong and J. A. Porco, *J. Am. Chem. Soc.*, 2016, **138**, 798–801.

28 (a) B. Machura, M. Wolff, E. Benoist, J. A. Schachner, N. C. Mösch-Zanetti, K. Takao and Y. Ikeda, *Polyhedron*, 2014, **69**, 205–218; (b) J. A. Schachner, B. Terfassa, L. M. Peschel, N. Zwettler, F. Belaj, P. Cias, G. Gescheidt and N. C. Mösch-Zanetti, *Inorg. Chem.*, 2014, **53**, 12918–12928; (c) S. C. A. Sousa, J. R. Bernardo, M. Wolff, B. Machura and A. C. Fernandes, *Eur. J. Org. Chem.*, 2014, 1855–1859; (d) B. Machura, M. Wolff, E. Benoist, J. A. Schachner and N. C. Mösch-Zanetti, *Dalton Trans.*, 2013, **42**, 8827–8837.

29 N. A. Milas and A. Golubovic, *J. Am. Chem. Soc.*, 1959, **81**, 6461–6462.

30 R. A. Sheldon, *Chem. Commun.*, 2008, **44**, 3352.

31 N. Zwettler, J. A. Schachner, F. Belaj and N. C. Mösch-Zanetti, *Inorg. Chem.*, 2014, **53**, 12832–12840.

32 J. A. Schachner, F. Belaj and N. C. Mösch-Zanetti, *Dalton Trans.*, 2020, **49**, 11142–11149.

33 D. V. Deubel, G. Frenking, P. Gisdakis, W. A. Herrmann, N. Rösch and J. Sundermeyer, *Acc. Chem. Res.*, 2004, **37**, 645–652.

34 J. A. Schachner, B. Berner, F. Belaj and N. C. Mösch-Zanetti, *Dalton Trans.*, 2019, **48**, 8106–8115.

35 G. Rouschias and G. Wilkinson, *J. Chem. Soc. A*, 1967, 993–1000.

36 *Rigaku Oxford Diffraction, CrysAlisPro:PX018*, Rigaku Corporation, 2024.

37 Bruker AXS Inc., *APEX2*, Bruker, Madison, Wisconsin, USA, 2014.

38 Bruker AXS Inc., *SADABS*, Bruker, Madison, Wisconsin, USA, 2016.

39 G. M. Sheldrick, *Acta Crystallogr., Sect. A:Found. Adv.*, 2015, **71**, 3–8.

40 O. V. Dolomanov, L. J. Bourhis, R. J. Gildea, J. A. K. Howard and H. Puschmann, *J. Appl. Crystallogr.*, 2009, **42**, 339–341.

41 G. M. Sheldrick, *Acta Crystallogr., Sect. C:Struct. Chem.*, 2015, **71**, 3–8.